Modulation of Luminescent Properties of Cocrystals Composed of Amino Substituted Dimethyl Phthalates and 1,2,4,5-Tetracyanobenzene by Crystal Engineering

Xiaokai Zhang [a, b‡], *Zhonghua Li* [a, c‡], *Rui Han* [a, b], *Jiawei Lin* [a, b], *Maolin Li* [a, b], *Jianmin Zhou* [a, b], *Songgu Wu* [a, b*], and *Junbo Gong* [a, b]

a. State Key Laboratory of Chemical Engineering, School of Chemical Engineering and Technology, Tianjin University, Tianjin 300072, People's Republic of China.
b. Haihe Laboratory of Sustainable Chemical Transformations.
c. Sinopec Research Institute of Petroleum Processing Co., Ltd., Beijing 100083, People's Republic of China.

Experimental section

Materials. Dimethyl 4-aminoisophthalate (DM4AI, purity 95%) was purchased from Shanghai Bide Pharmaceutical Technology Co., Ltd. Dimethyl aminoterephthalate (DMAT, purity 98%), dimethyl 5-aminoisophthalate (DM5AI, purity 98%), and 1,2,4,5-tetracyanobenzene (TCNB, purity 98%) were purchased from Tianjin Heowns Biochemical Technology Co., Ltd. Methanol (purity 99.5%), n-hexane (purity 97.0%), acetonitrile (purity 99.8%) and acetone (purity 99.5%) purchased from Tianjin Jiangtian Chemical Technology Co., Ltd. All chemicals were used directly without further purification.

Preparation of crystals.

DM4AI. 20 mg of DM4AI were weighed and dissolved in a mixture of 1 ml n-hexane and 0.5 ml acetone. Evaporation of the solution in a dark environment at 10 ℃ and colorless massive crystals were obtained within 3 days.

DMAT and DM5AI. The crystallization experiments and single-crystal structures of DMAT and DM5AI have been reported.[1, 2]

DM4AI-TCNB. DM4AI and TCNB were taken in 1:1 molar ratio and ground in a mortar for about 10 minutes assisted with a few drops of methanol. And then 15 mg of the mixture were dissolved in 1 mL of methanol and 10 drops of acetonitrile. Evaporation of the solution in a dark environment at 10 ℃ and flaky yellow crystals were obtained within three days.

DMAT-TCNB. DMAT and TCNB were taken in 1:1 molar ratio and ground in a mortar for about 10 minutes assisted with a few drops of methanol. And then 15 mg of the mixture were dissolved in 0.5 mL of methanol and 0.5 mL of acetonitrile. Evaporation of the solution in a dark environment at 10 ℃ and two types of crystals, flake orange crystals (DMAT-TCNB-O) and flake yellow crystals (DMAT-TCNB-Y), were obtained within one week.

DM5AI-TCNB. DM5AI and TCNB were taken in 1:1 molar ratio and ground in a mortar for about 10 minutes assisted with a few drops of acetone. And then 10 mg of the mixture were dissolved in 0.5 mL of methanol and 0.5 mL of acetonitrile.

Evaporation of the solution in a dark environment at 10 ℃ and flaky orange crystals were obtained within one week.

Characterization techniques. The powder X-ray diffraction (PXRD) data was obtained through a Rigaku D/MAX-2500 X-ray diffractometer with Cu Kα radiation (λ = 1.54178 Å). The voltage of the generator was set to 40 kV, and the current was 100 mA. At ambient temperature, the PXRD data of the cocrystals in the 2θ range of 2−35° was collected at a scan rate of 8°/min. Jade 6.5 software was used to compare and analyze the PXRD patterns. The single-crystal X-ray diffraction (SCXRD) data of the cocrystals was obtained at 113.15 or 120 K on a Rigaku mm007 Saturn 944+ diffractometer with Mo Kα radiation (λ = 0.71073 Å). With Olex2,[3] the structure was solved using Intrinsic Phasing method of the SHELXT[4] structure solution program, and it is refined using Least Squares minimization of the SHELXL[5] refinement package. Mercury software[6] was used to simulate PXRD patterns, and analyze crystal packing patterns and non-covalent interactions. Under ambient conditions, the fourier transform infrared (FTIR) spectra of the cocrystals and the corresponding original components in the range of 4000 to 400 cm^{-1} were recorded on the Bruker Alpha FT-IR 750 spectrometer with a resolution of 4 cm^{-1}. The UV−vis absorption spectra of the cocrystals and the corresponding original components were recorded on a UV-3600i Plus spectrophotometer (Shimadzu, Japan). Thermogravimetric analysis (TGA) was performed using Mettler TGA/DSC STARe system. 5−10 mg sample was heated from 25 ℃ to the target temperature at a constant heating rate of 10 ℃/min, accompanied by a nitrogen purge at a flow rate of 20 mL/min. Differential scanning calorimetry (DSC) was carried out on a Mettler Toledo DSC 1/500 module. Samples of 5−10 mg were weighed and placed in a standard alumina crucible, and heated from 25 ℃ to the set temperature at a constant heating rate of 10 ℃/min under a nitrogen purge of 50 mL/min. Hot-stage microscopy (HSM) images were obtained using an Olympus BX-51 microscope equipped with a DSC600 hot-stage Linkam system. The cocrystal samples were heated at a constant heating rate of 10 ℃/min, and the HSM images were periodically obtained.

Luminescent properties test. The luminescent properties of the cocrystals and the donors were made with an Edinburgh FLS1000 luminescence spectrometer.

Computational studies. The analysis of the Hirshfeld surfaces and two-dimensional (2D) fingerprint plots was conducted using CrystalExplorer 21.5 program,[7] which can intuitively reflect the intermolecular interactions. The density functional theory (DFT) calculation was performed on Gaussian 09 packages at the level of B3LYP/6-31G (d, p).[8]

Table S1. Crystallographic information of the individual components.

Crystal	DM4AI	DMAT	DM5AI
Empirical formula	$C_{10}H_{11}NO_4$	$C_{10}H_{11}NO_4$	$C_{10}H_{11}NO_4$
Formula weight	209.20	209.20	209.20
Temperature/K	113.15	273.0	98.0
Crystal system	monoclinic	monoclinic	monoclinic
Space group	$P2_1/c$	$P2_1/c$	Pn
a/Å	10.0548(5)	4.7988(3)	9.6140(5)
b/Å	7.1932(4)	17.3121(13)	3.8690(2)
c/Å	14.2783(8)	11.8745(9)	13.7437(7)
α/°	90	90	90
β/°	108.473(5)	91.415(3)	105.913(2)
γ/°	90	90	90
Volume/Å^3	979.48(10)	986.20(12)	491.63(4)
Z	4	4	2
R_{int}	0.0452	0.0579	0.0280
R_1(I > 2sigma(I))	0.0558	0.0521	0.0435
wR_2	0.1475	0.1272	0.1116
Data completeness	0.926	0.999	1.91/0.96
GOF(S)	1.041	1.045	1.092
CCDC	2334584	2118365	2130382

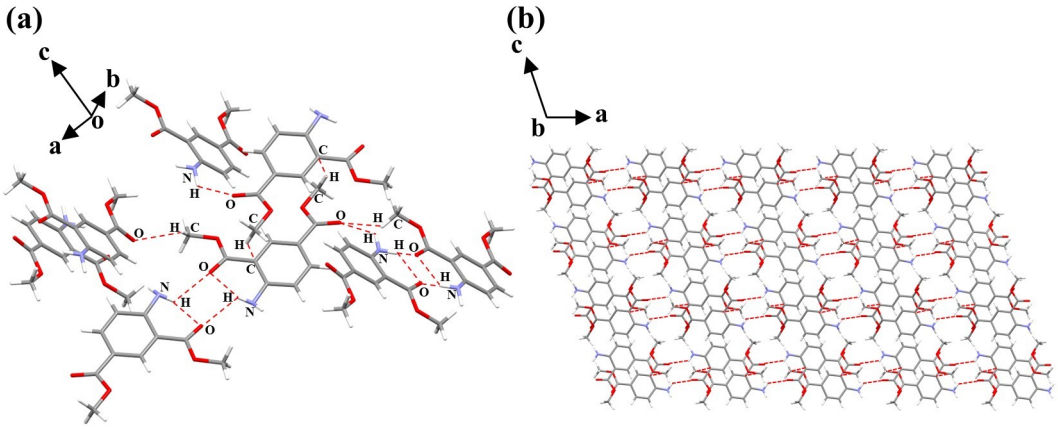

Figure S1. (a) Non-covalent bond interactions of DM4AI. (b) Packing pattern of DM4AI.

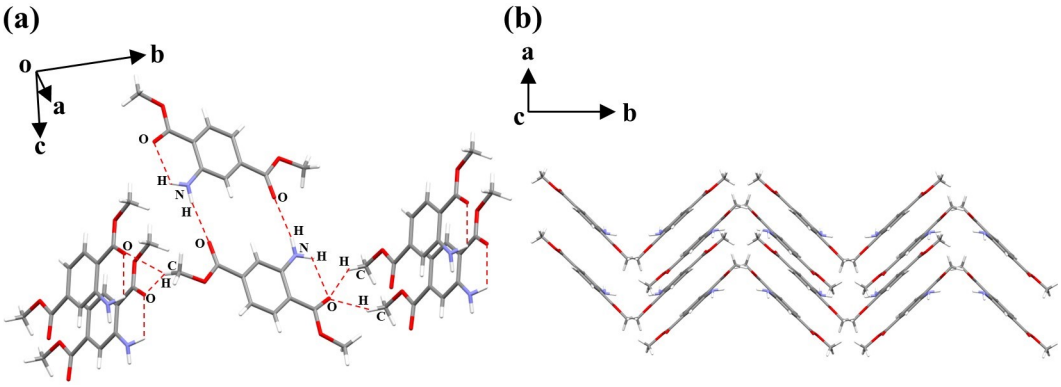

Figure S2. (a) Non-covalent bond interactions of DMAT. (b) Chain structure of DMAT.

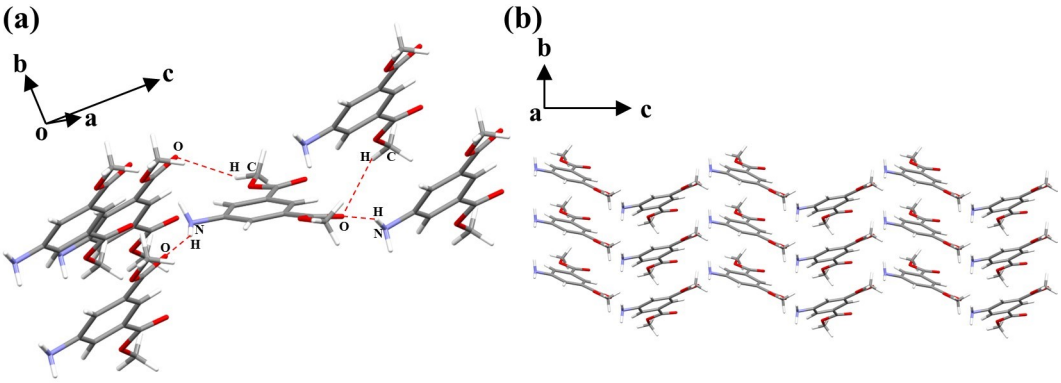

Figure S3. (a) Non-covalent bond interactions of DM5AI. (b) Chain structure of DM5AI.

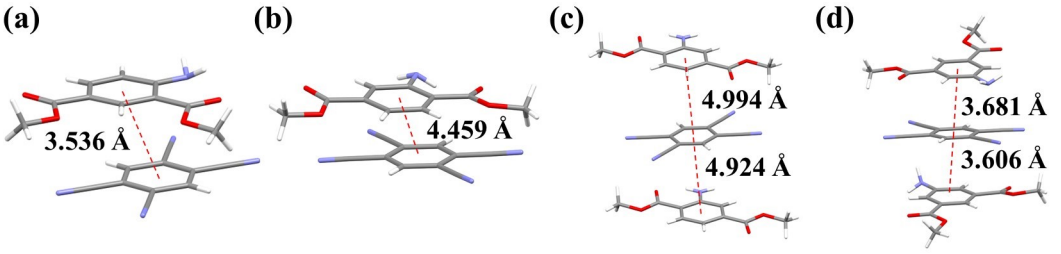

Figure S4. The distances of the centroid π–π interaction in (a) DM4AI-TCNB, (b) DMAT-TCNB-O, (c)DMAT-TCNB-Y and (d) DM5AI-TCNB.

Table S2. Non-covalent bond interactions in the molecular layer of DM4AI-TCNB.

D−H···A Interactions	D−H(Å)	H···A(Å)	∠D−H···A(°)
N3−H3B···O3	0.881	2.097	123.48
C15−H15A···O3	0.980	2.658	110.70
C15−H15B···N1	0.980	2.749	134.68
N3−H3A···N2	0.881	2.414	142.68
C8−H8···N2	0.950	2.635	158.12
C3−H3···O1	0.950	2.202	165.17

Table S3. Non-covalent bond interactions in the molecular layer of DMAT-TCNB-O.

D−H···A Interactions	D−H(Å)	H···A(Å)	∠D−H···A(°)
N1−H1A···O3	0.880	2.117	123.77
N1−H1B···O1	0.881	2.104	168.48
N1−H1A···N2	0.880	2.613	111.06
C13−H13···O3	0.950	2.272	159.99
C1−H1C···N2	0.980	2.607	144.54
C8−H8···H8	0.950	2.221	154.64
C1−H1E···C6	0.980	2.845	125.18
C1−H1E···C7	0.980	2.790	151.23

Table S4. Non-covalent bond interactions in the molecular layer of DMAT-TCNB-Y.

D−H···A Interactions	D−H(Å)	H···A(Å)	∠D−H···A(°)
N4−H4B···O	0.880	1.957	129.25
C−HA···O3	0.980	2.641	148.11
C8−H8B···O1	0.980	2.556	156.43
C14−H14···O	0.950	2.355	153.00
N4−H4B···N	0.880	2.540	132.55
N4−H4A···N18	0.881	2.181	166.75
C4−H4···O2	0.950	2.315	155.58
C−HC···C6	0.980	2.846	134.06
C−HB···N1	0.980	2.749	129.51
C8−H8A···N	0.980	2.644	138.52

Table S5. Non-covalent bond interactions in the molecular layer of DM5AI-TCNB.

D−H···A Interactions	D−H(Å)	H···A(Å)	∠D−H···A(°)
C3−H3···O8	0.950	2.486	145.15
C15−H15···O2	0.950	2.469	145.40
N2−H2B···O2	0.861	2.488	139.84
C13−H13···N5	0.950	2.649	156.48
C23−H23···O6	0.950	2.128	155.91
C5−H5···N3	0.950	2.594	161.37
C26−H26···O4	0.950	2.149	153.81
C9−H9B···O3	0.980	2.649	128.29
C19−H19B···N4	0.980	2.685	137.54
C9−H9C···O5	0.980	2.611	131.23
C17−H17B···O3	0.980	2.669	134.31
N1−H1B···H2A	0.863	2.258	129.98
N1−H1A···C24	0.864	2.775	131.78
N1−H1A···C25	0.864	2.572	136.09
N1−H1A···C29	0.864	2.871	139.12
N1−H1A···C30	0.864	2.483	151.62

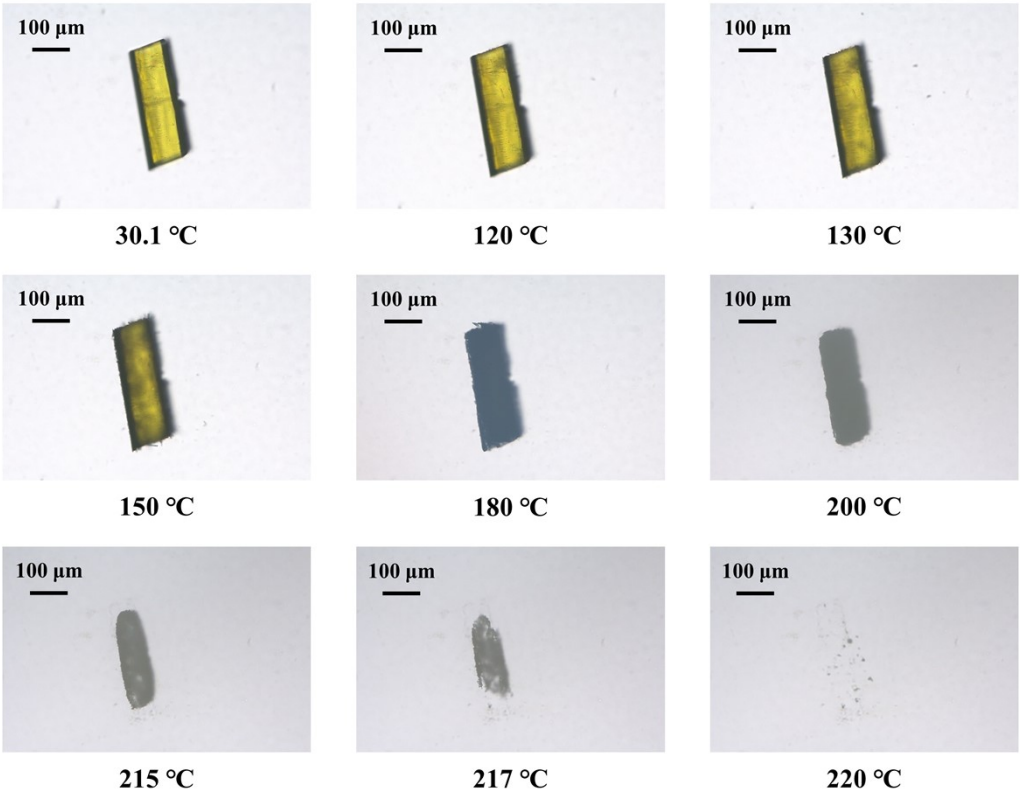

Figure S5. HSM images for DM4AI-TCNB.

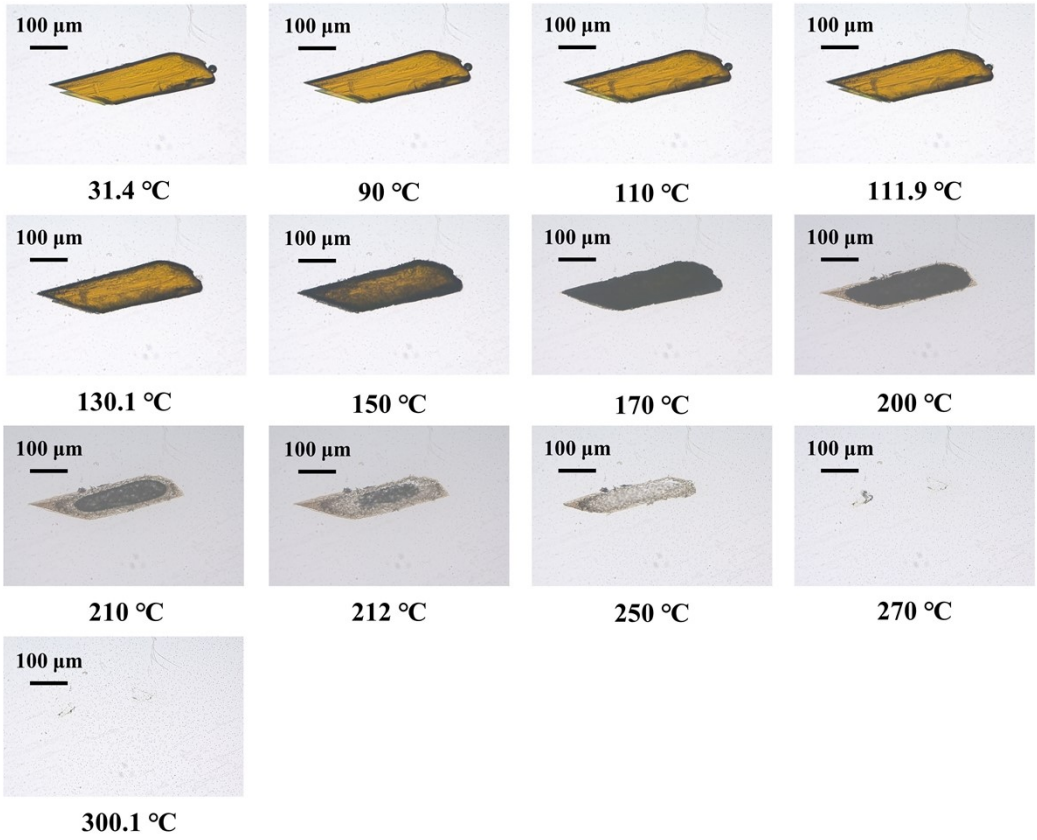

Figure S6. HSM images for DMAT-TCNB-O.

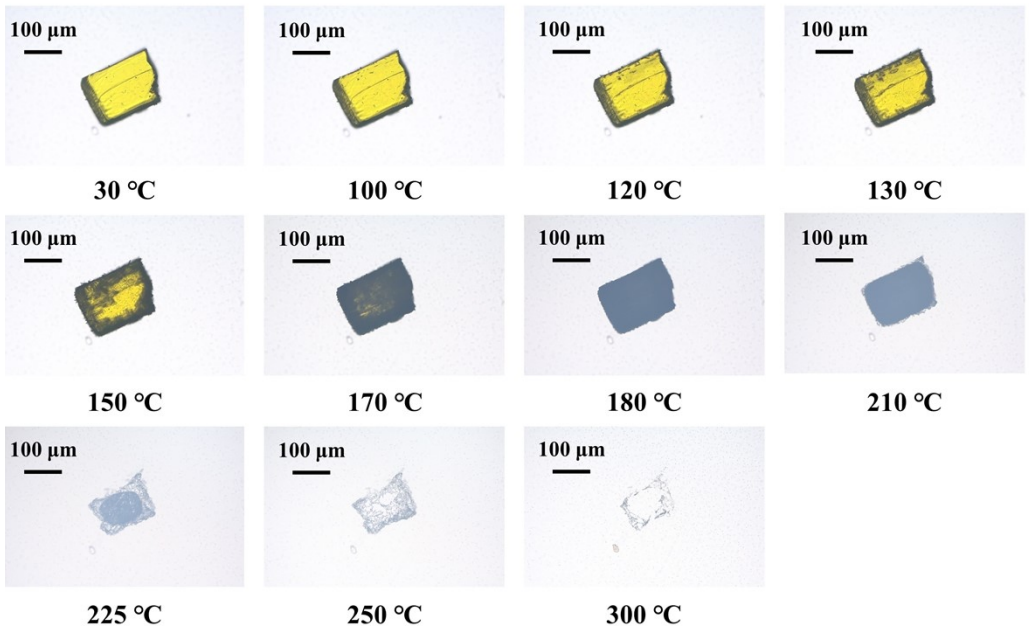

Figure S7. HSM images for DMAT-TCNB-Y.

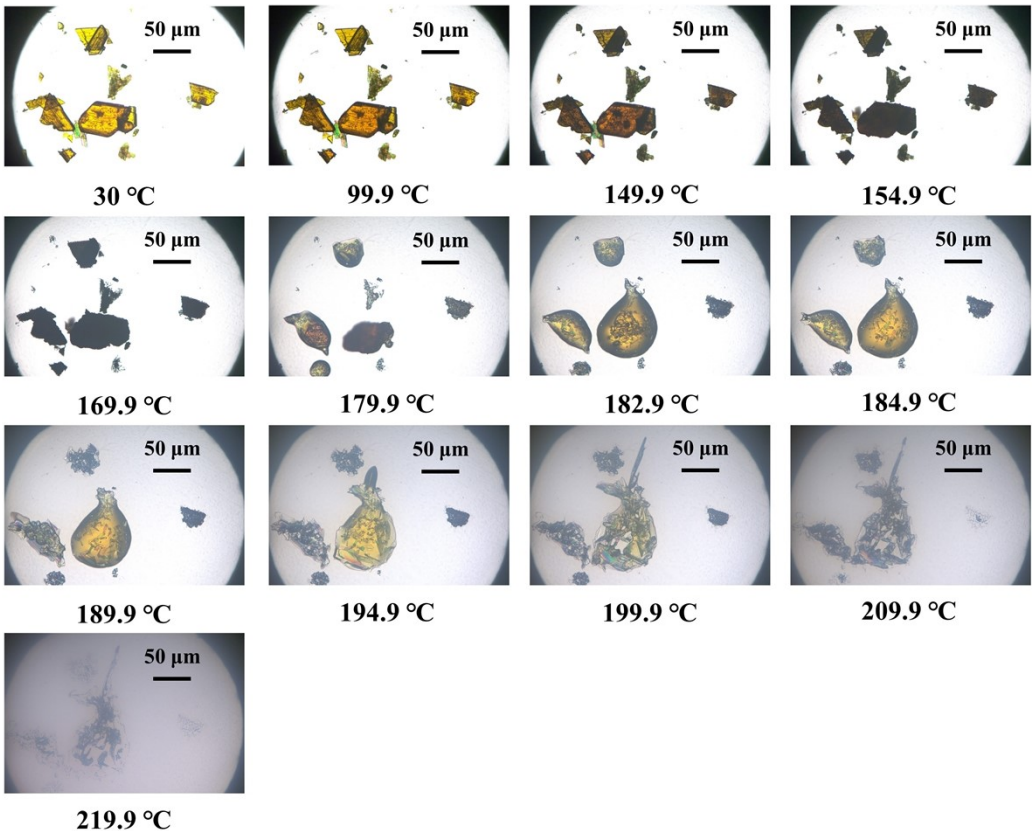

Figure S8. HSM images for DM5AI-TCNB.

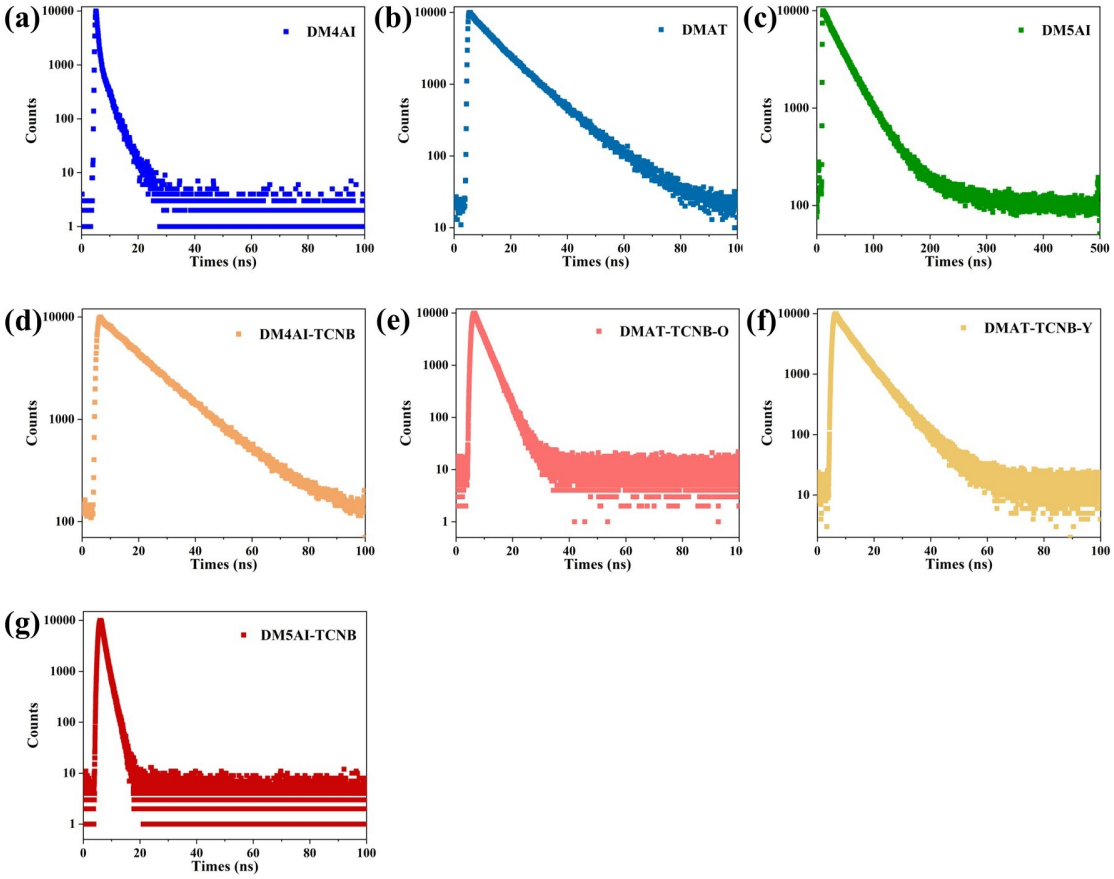

Figure S9. Fluorescence decay curves of the cocrystals and the corresponding original components.

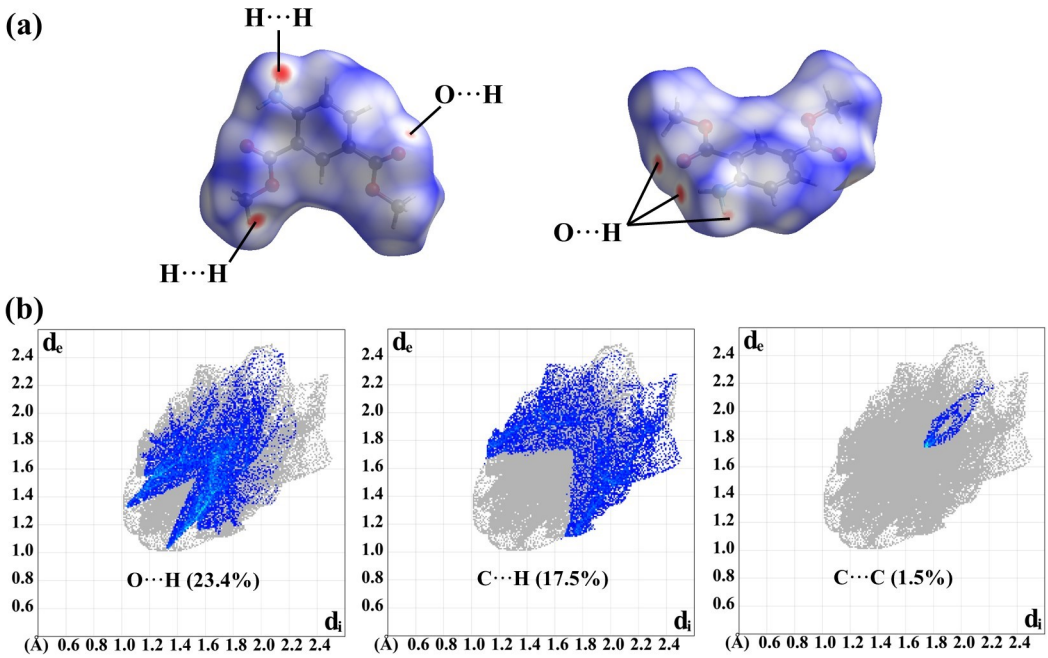

Figure S10. (a) Hirshfeld surface of DM4AI. (b)2D fingerprint plots of DM4AI molecule.

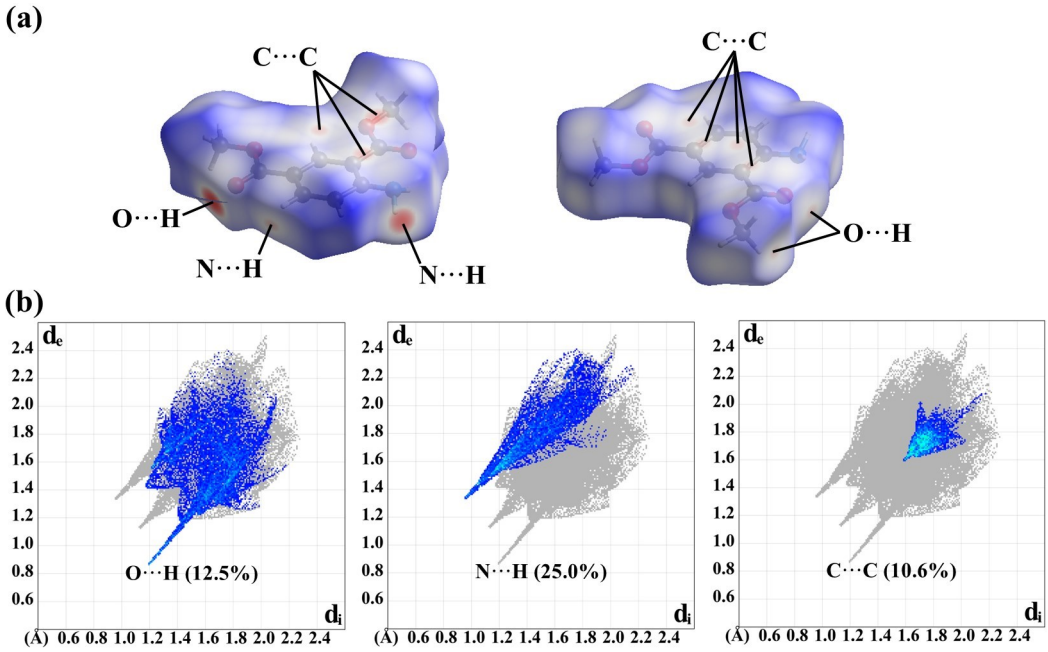

Figure S11. (a) Hirshfeld surface of DM4AI-TCNB. (b)2D fingerprint plots of DM4AI molecule in cocrystal DM4AI-TCNB.

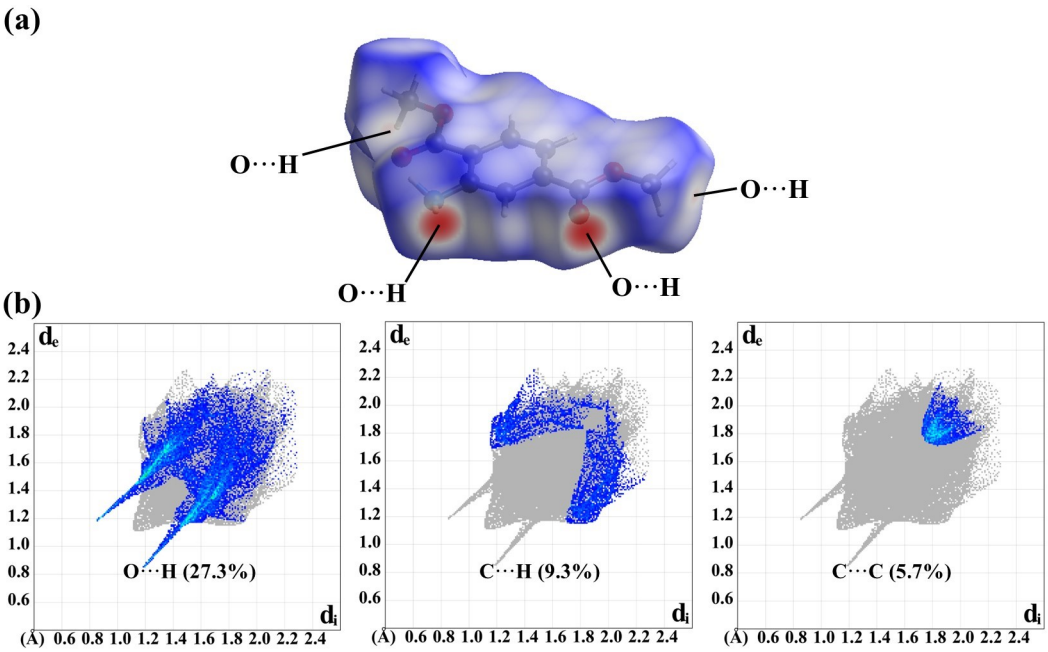

Figure S12. (a) Hirshfeld surface of DMAT. (b)2D fingerprint plots of DMAT molecule.

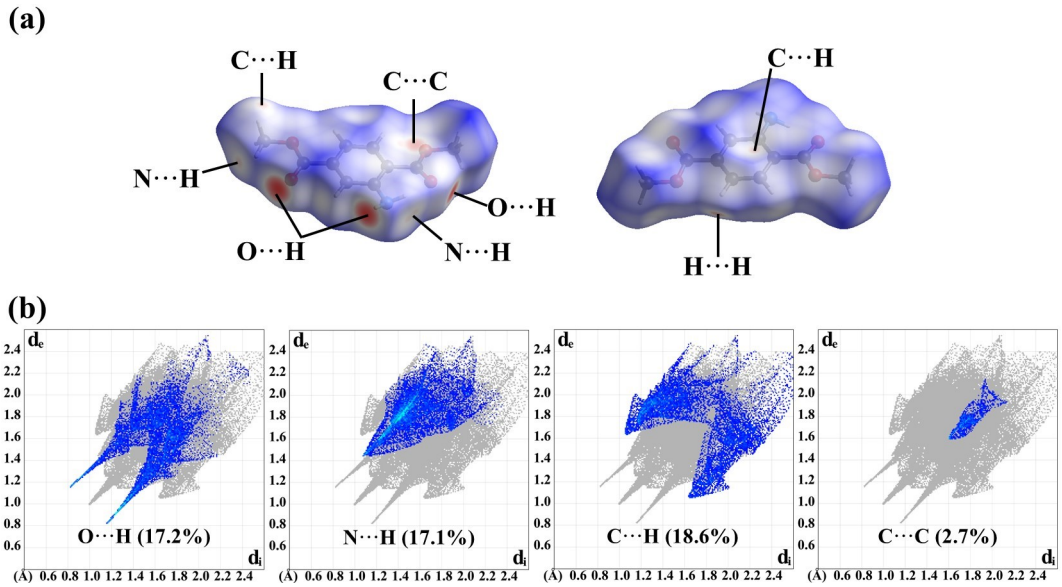

Figure S13. (a) Hirshfeld surface of DMAT-TCNB-O. (b)2D fingerprint plots of DMAT molecule in cocrystal DMAT-TCNB-O.

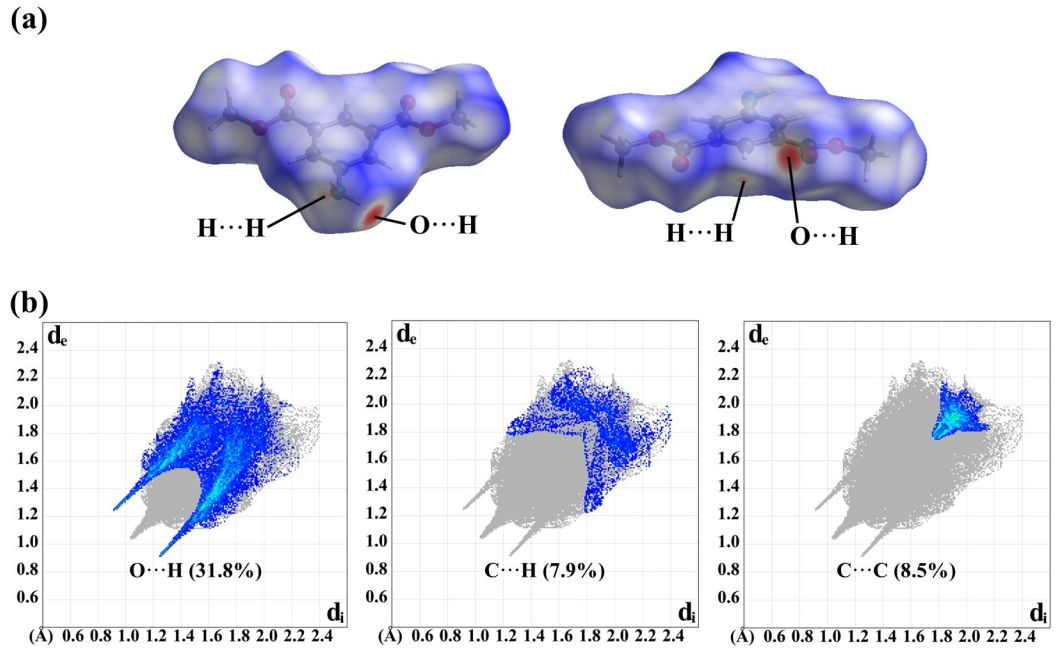

Figure S14. (a) Hirshfeld surface of DM5AI. (b)2D fingerprint plots of DM5AI molecule.

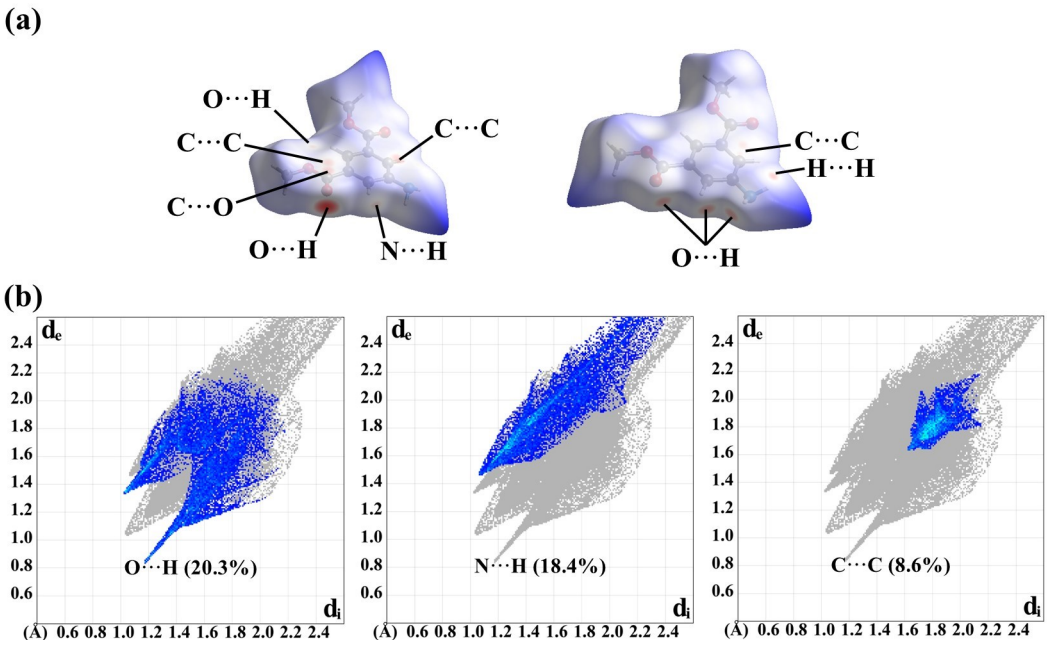

Figure S15. (a) Hirshfeld surface of DM5AI-TCNB. (b)2D fingerprint plots of DM5AI molecule in cocrystal DM5AI-TCNB.

References

1. B. L. Tang, M. J. Li, X. Yu and H. Y. Zhang, *J. Mater. Chem. C*, 2022, **10**, 3894-3900.
2. B. L. Tang, X. Yu and H. Y. Zhang, *Acta Polym. Sin.*, 2021, **52**, 1015-1023.
3. O. V. Dolomanov, L. J. Bourhis, R. J. Gildea, J. A. K. Howard and H. Puschmann, *J. Appl. Crystallogr.*, 2009, **42**, 339-341.
4. G. M. Sheldrick, *Acta Crystallogr. Sect. A*, 2015, **71**, 3-8.
5. G. M. Sheldrick, *Acta Crystallogr. Sect. C-Struct. Chem.*, 2015, **71**, 3-8.
6. C. F. Macrae, P. R. Edgington, P. McCabe, E. Pidcock, G. P. Shields, R. Taylor, M. Towler and J. van De Streek, *J. Appl. Crystallogr.*, 2006, **39**, 453-457.
7. P. R. Spackman, M. J. Turner, J. J. McKinnon, S. K. Wolff, D. J. Grimwood, D. Jayatilaka and M. A. Spackman, *J. Appl. Crystallogr.*, 2021, **54**, 1006-1011.
8. H. Zhang, D. Q. Lin, M. Z. Wu, D. Jin, L. Huang and L. H. Xie, *Cryst. Growth Des.*, 2023, **23**, 6548-6556.